

Numerical Simulation of Flow Past a Circular Cylinder Undergoing Figure-eight-Type Motion: Oscillation Amplitude Effect

Qasem M. Al-Mdallal

Abstract—This paper presents a computational study of laminar, viscous incompressible flow past a circular cylinder undergoing figure-eight-type motion using the two-dimensional Navier-Stokes equations. The numerical method is based on Fourier spectral method together with finite difference approximations. The response of the flow are investigated at a fixed Reynolds number, $R = 200$. The oscillation frequency was fixed to the vortex shedding frequency from a fixed cylinder, f_0 , while the amplitudes of oscillations were varied from 0.1 to $1.0a$, where a represents the radius of the cylinder. The response of the flow through the fluid forces acting on the surface of the cylinder are investigated.

Index Terms—lock-on; streamwise oscillation; transverse oscillation; figure-eight-type motion; fluid forces.

I. INTRODUCTION

VORTEX-shedding from oscillating bluff bodies is an important engineering problem because it is associated with the surface fluid forces. Hence, many researchers had discussed this problem with different types of oscillatory motions. However, the problem of flow past a cylinder performing one-degree of freedom (1-DoF) forced streamwise or transverse oscillation is discussed by many researchers (see the recent works by Al-Mdallal [1]; Al-Mdallal et al. [2]; Barrero-Gil and Fernandez-Arroyo [3]; Carmo et al. [4]; Konstantinidis and Liang [5]; Marzouk and Nayfeh [6]; Suthon and Dalton [7] and the references therein). However, there is only very few studies have focused on the problem of flow past a circular cylinder with combined two-degree of freedom (2-DoF) streamwise and transverse oscillation (we may refer the reader to Al-Mdallal [8], [9] Baranyi [10]; Didier and Borges [11]; Stansby and Rainey [12]; Williamson et al. [13]). The problem of a circular cylinder undergoing a figure-eight-type motion, which is a special case of combined two-degree of freedom (2-DoF) streamwise and transverse oscillation, in a uniform stream was also received some attention in few studies; see for example Jeon and Gharib [14] and Reid [15] and Baranyi [16]. Therefore, this problem is considered in the present study.

This paper is organized as follows. The governing equations for the physical model are presented in section II. In section III, we describe the numerical approach employed to obtain the numerical solution. In section IV, numerical simulation results are discussed. Finally, concluding remarks are highlighted in section V.

Manuscript received February 25, 2013; revised March 26, 2013.

Q.M. Al-Mdallal is with the Department of Mathematical Sciences, United Arab Emirates University, P.O. Box 15551, Al Ain, Abu Dhabi, UAE e-mail: q.almdallal@uaeu.ac.ae

II. COMPUTATIONAL FLOW MODEL

The cylinder, whose axis coincides with the z -axis, is placed horizontally in a cross-stream of an infinite extend where the flow of a viscous incompressible fluid of constant velocity U past the cylinder in the positive x -direction. The cylinder is at rest and at $t = 0$ it suddenly starts to move with combined two-degree of freedom (2-DoF) streamwise and transverse oscillation forming a figure-eight-type motion. The imposed streamwise and transverse oscillatory motions are, respectively, described by

$$X(t) = A_x \sin(2\pi f_x t), \quad Y(t) = A_y \sin(2\pi f_y t), \quad (1)$$

where A_x and A_y ; f_x and f_y are, respectively, the dimensionless amplitudes and frequencies of the two simple harmonic motions. To create a figure-8-type motion with a clockwise orientation, we assume that $f_y = 2f_x$. In this study, we assume that $A = A_x = A_y$.

III. NUMERICAL APPROACH

The governing equations for two-dimensional unsteady incompressible viscous flow in terms of the vorticity, ζ , and stream function, ψ , in dimensionless form are given by

$$e^{2\xi} \frac{\partial \zeta}{\partial t} = \frac{2}{R} \left(\frac{\partial^2 \zeta}{\partial \xi^2} + \frac{\partial^2 \zeta}{\partial \theta^2} \right) + \frac{\partial \psi}{\partial \xi} \frac{\partial \zeta}{\partial \theta} - \frac{\partial \psi}{\partial \theta} \frac{\partial \zeta}{\partial \xi}, \quad (2)$$

$$\frac{\partial^2 \psi}{\partial \xi^2} + \frac{\partial^2 \psi}{\partial \theta^2} = e^{2\xi} \zeta. \quad (3)$$

using the modified polar coordinate (ξ, θ) system where $\xi = \ln(r)$. Here $r = \sqrt{x^2 + y^2}$ represents the dimensionless radial coordinate. Note that, a frame of reference is used in which the axes translate and oscillate with the cylinder. Here The boundary conditions for ψ and ζ are based on the no-slip and impermeability conditions on the cylinder and the free stream condition away from it. These conditions are utilized to derive sets of integral conditions on ζ by applying one of the Green's identities to the domain of the field of flow, for more details see Dennis and Chang [17], [18]. Further, all flow variables must be periodic functions of the angular coordinate θ with period 2π . In summary, the associated conditions with equations (2) and (3) are

$$\psi = \frac{\partial \psi}{\partial \xi} = 0, \quad \text{when } \xi = 0, \quad (4)$$

$$\int_0^\infty \int_0^{2\pi} e^{(2-p)\xi} \zeta(\xi, \theta, t) \cos(p\theta) d\theta d\xi = 2\pi \dot{Y}(t) \delta_{1,p}, \quad (5a)$$

$$\int_0^\infty \int_0^{2\pi} e^{(2-p)\xi} \zeta(\xi, \theta, t) \sin(p\theta) d\theta d\xi = 2\pi(1-\dot{X}(t))\delta_{1,p} \quad (5b)$$

$$\zeta \rightarrow 0 \quad \text{as } \xi \rightarrow \infty. \quad (6)$$

$$\zeta(\xi, \theta, t) = \zeta(\xi, \theta + 2\pi, t), \quad \psi(\xi, \theta, t) = \psi(\xi, \theta + 2\pi, t). \quad (7)$$

Notice that $p \in \{0, 1, \dots\}$, where $\delta_{1,p} = 1$ if $n = 1$; $\delta_{1,p} = 0$ if $n \neq 1$.

The numerical method of solution was initially developed by Collins and Dennis [19] and has been successfully implemented to simulations of flows past oscillating cylinders [see for example, Badr and Dennis [20], Badr et al. [21], Dennis et al. [22], Mahfouz and Badr [23], Kocabiyik et al. [24], Lawrence [25], Al-Mdallal [1], Al-Mdallal and Kocabiyik [26] and Al-Mdallal et al. [2]]. The numerical method is based on Fourier spectral method together with finite difference approximations. Note that the computational domain along ξ direction is unbounded, hence we choose an artificial outer boundary, $\xi_\infty = 7$, for the numerical treatment. The finite difference schemes require dividing the space computational domain $[0, \xi_\infty]$ into $M + 1$ equal subintervals whose endpoints are the mesh points $\xi_i = ih$ for $i = 0, 1, \dots, M + 1$ where $h = \frac{\xi_{M+1}}{M+1}$ represents the uniform grid step. Further, we set Δt_{j+1} be a non-uniform time increment given by $\Delta t_{j+1} = t_{j+1} - t_j$, where $j = 1, 2, \dots$ and $t_1 = 0$. Hence, for each time step t_{j+1} we need to determine the solutions at the mesh points ξ_i , for $i = 0, 1, \dots, M + 1$.

The simulations are carried out by using the time step $\Delta t_{j+1} = 10^{-4}$ for the first 100 steps, then was increased to $\Delta t_{j+1} = 10^{-3}$ for the next 100 steps and finally $\Delta t_{j+1} = 10^{-2}$ for the rest of the calculations. The number of points in the ξ direction is taken as 349 with a grid size of $\Delta z = 0.02$. The maximum number of terms in the Fourier series is taken as $N = 60$ for all cases considered in this paper.

Numerical simulations via C++ were carried out on 4 Dell Blade Servers. Each server has a PE M600 Quad Core Xeon E5450 processor, 2 X 146 GB SAS HD, 8 CPU x2.992 Ghz, and 8 GB RAM, located in the Department of Physics at United Arab Emirates University.

IV. NUMERICAL SIMULATION RESULTS

The full set of results for the cases of $R = 200$: $f/f_0 = 0.5 - 4$ when $0 \leq A \leq 1.0$ will be reported elsewhere, but here we concentrate and analyze only for the cases when $A = 0.1 - 1.0$ and $f/f_0 = 1.0$. The predicted value for the natural shedding frequency f_0 by the present simulation at $R = 200$ is 0.0977.

The time history of the lift coefficients in the domain $60 \leq t \leq 140$ are shown in Figure 1 for the case of $R = 200$, $f_x/f_0 = 1.0$ and $0.1 \leq A \leq 1.0$. It is clearly seen that when $A \leq 2.0$, the lift coefficient shows a semi-repetitive signature every one period of streamwise oscillation, T_x . This inspire us to conclude that the vortex

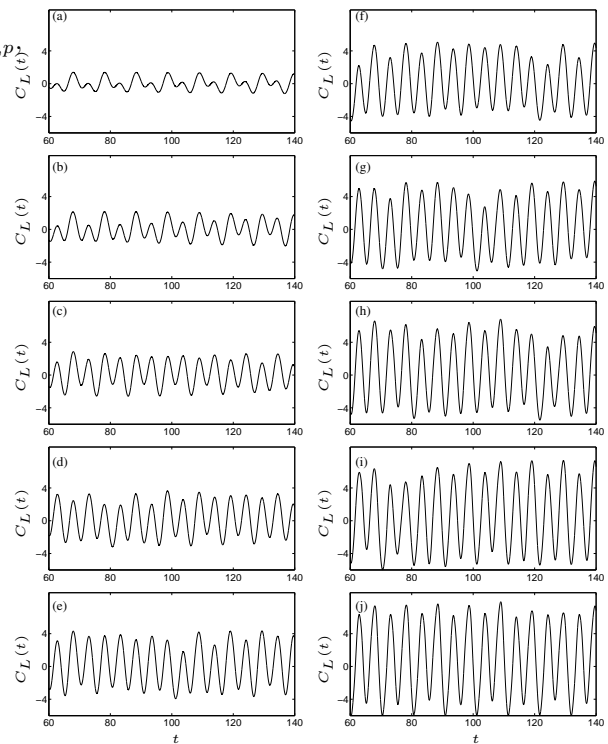


Fig. 1. The time variation of C_L for $R = 200$, $f/f_0 = 1.0$: (a) $A = 0.1$, (b) $A = 0.2$, (c) $A = 0.3$, (d) $A = 0.4$, (e) $A = 0.5$, (f) $A = 0.6$, (g) $A = 0.7$, (h) $A = 0.8$, (i) $A = 0.9$, (j) $A = 1.0$.

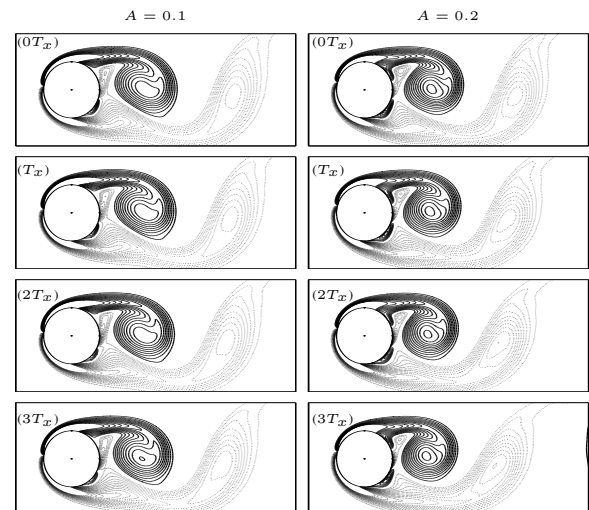


Fig. 2. Equivorticity lines at an instant corresponding to the cylinder displacement $(X(t), Y(t)) = (0, 0)$ over 4 periods of streamwise oscillations, $4T_x$, for $R = 200$, $A = 0.1, 0.2$ and $f/f_0 = 1.0$ (quasi-locked on regime).

shedding in the near-wake region is quasi-locked-on in this range.

To support this conclusion, Figure 2 displays a series of instantaneous equivorticity contours over four forcing periods for $R = 200$, $A = 0.1, 0.2$ and $f/f_0 = 1.0$. The snapshots are taken at the instant $(X(t), Y(t)) = (0, 0)$ and every one full cycle of streamwise oscillation thereafter. It is evident from this figure that the near-wake frequency is almost but not completely locked-on to the cylinder oscillation frequencies. Notice that the size of the shedding vortices decreases as the oscillation amplitude increases. A final remark on Figure 2 is that the vortex shedding produces the quasi-locked-on **2S** mode per T_x , in which two vortices are shed alternatively from both sides of the cylinder over T_x .

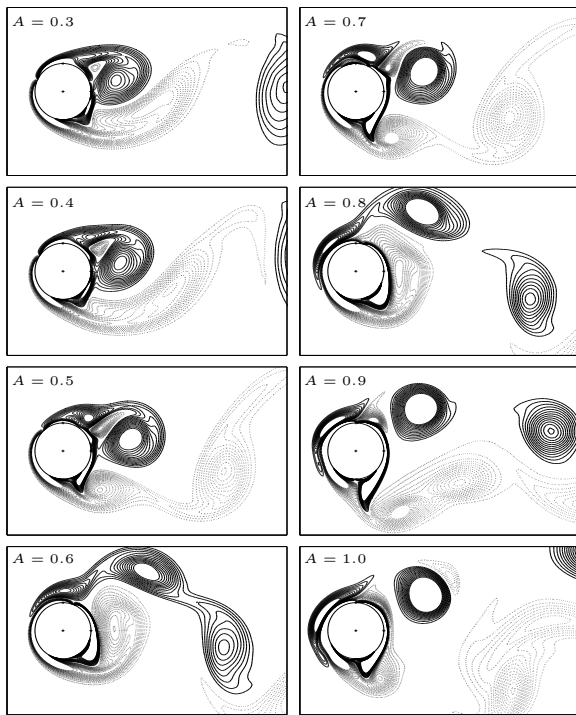


Fig. 3. Equivorticity lines at an instant corresponding to the cylinder displacement $(X(t), Y(t)) = (0, 0)$ ($t = 92.12$), for $R = 200$, $A = 0.3 - 1.0$ and $f/f_0 = 1.0$ (non-lock on regime).

A remarkable conclusion is that: as the oscillation amplitude increases beyond 0.2, the vortex shedding becomes more complicated due to the strong interaction between the body of the cylinder and the surrounding fluid. This interaction causes the development of several secondary vortices on both sides of the cylinder as well as the occurrence of the coalescence phenomenon in the near wake region as shown in Figure 3. Moreover, it is noted a separated region forms at the front part of the cylinder surface at relatively high values of oscillation amplitude ($A \geq 0.6$).

Table I shows the predicted values of the maximum lift coefficient, $C_{L,max}$, the minimum lift coefficient, $C_{L,min}$, the RMS lift coefficient, $C_{L,rms}$, the mean lift coefficient, \widehat{C}_L , the maximum drag coefficient, $C_{D,max}$, the minimum drag coefficient, $C_{D,min}$, the RMS drag coefficient, $C_{D,rms}$, the mean drag coefficient, \widehat{C}_D , the maximum moment coefficient, $C_{M,max}$, the minimum moment coefficient, $C_{M,min}$, the RMS moment coefficient, $C_{M,rms}$ and the mean moment coefficient, \widehat{C}_M for the case of $R = 200$, $f/f_0 = 1.0$ and $0.1 \leq A \leq 1.0$. It is clearly seen that the quantities $C_{L,max}$, $C_{D,max}$, $C_{L,rms}$, $C_{D,rms}$ and $C_{M,rms}$ are strictly increasing as the oscillation amplitude, A , increases. However, we notice that $C_{L,min}$, $C_{D,min}$ and $C_{M,min}$ are strictly decreasing with the increase of A . Therefore, we may report that magnitudes of drag, lift and moment coefficients are increasing as the oscillation amplitude, A , increases. On the other hand, it is notable that the quantities \widehat{C}_L and \widehat{C}_D have a trend to increase as A increases.

V. CONCLUSION

The problem of flow past an oscillation cylinder in a figure-8-type motion is investigated numerically. The numerical method is based on Fourier spectral method

together with finite difference approximations. Quasi-lock-on modes were verified at low oscillation amplitudes. The effect of increasing the oscillation amplitude on the lift, drag and moment coefficients is also investigated.

ACKNOWLEDGEMENTS

The author would like to express his appreciation for the Faculty of Science at United Arab Emirates University for providing the computing facilities that this research heavily depend upon. In addition, the author would like to extend his thanks to Engineer Naser Mushtaha of the United Arab Emirates University for his valuable technical support.

REFERENCES

- [1] Q. Al-Mdallal, "Analysis and computation of the cross-flow past an oscillating cylinder with two degrees of freedom," Ph.D. dissertation, Memorial University of Newfoundland, St. John's, Canada, 2004.
- [2] Q. Al-Mdallal, K. P. Lawrence, and S. Kocabiyik, "Forced streamwise oscillations of a circular cylinder: lock-on modes and resulting forces," *Journal of Fluids and Structures*, vol. 23, no. 5, pp. 681–701, 2007.
- [3] A. Barrero-Gil and P. Fernandez-Arroyo, "Fluid excitation of an oscillating circular cylinder in cross-flow," *European Journal of Mechanics - B/Fluids*, vol. 29, no. 5, pp. 364–368, 2010.
- [4] B. Carmo, S. Sherwin, P. Bearman, and R. Willden, "Flow-induced vibration of a circular cylinder subjected to wake interference at low Reynolds number," *Journal of Fluids and Structures*, vol. 27, no. 4, pp. 503–522, 2011.
- [5] E. Konstantinidis and C. Liang, "Dynamic response of a turbulent cylinder wake to sinusoidal inflow perturbations across the vortex lock-on range," *Physics of Fluids*, vol. 23, no. 7, p. In Press, 2011.
- [6] O. A. Marzouk and A. H. Nayfeh, "Characterization of the flow over a cylinder moving harmonically in the cross-flow direction," *International Journal of Non-Linear Mechanics*, vol. 45, no. 8, pp. 821–833, 2010.
- [7] P. Suthon and C. Dalton, "Streakline visualization of the structures in the near wake of a circular cylinder in sinusoidally oscillating flow," *Journal of Fluids and Structures*, vol. 27, no. 7, pp. 885–902, 2011.
- [8] Q. Al-Mdallal, "On the numerical simulation of flow past an oscillating circular cylinder in a circular path: Oscillation amplitude effect," *World Academy of Science, Engineering and Technology*, vol. 64, pp. 1042–1045, 2012.
- [9] Q. Al-Mdallal, "A numerical study of initial flow past a circular cylinder with combined streamwise and transverse oscillations," *Computers and Fluids*, vol. 63, pp. 174–183, 2012.
- [10] L. Baranyi, "Numerical simulation of flow around an orbiting cylinder at different ellipticity values," *Journal of Fluids and Structures*, vol. 24, no. 7, pp. 883–906, 2008.
- [11] E. Didier and A. R. J. Borges, "Numerical predictions of low Reynolds number flow over an oscillating circular cylinder," *Journal of Computational and Applied Mechanics*, vol. 8, no. 1, pp. 39–55, 2007.
- [12] P. K. Stansby and R. C. T. Rainey, "On the orbital response of a rotating cylinder in a current," *Journal of Fluid Mechanics*, vol. 439, pp. 87–108, 2001.
- [13] C. H. K. Williamson, P. Hess, M. Peter, and R. Govardhan, "Fluid loading and vortex dynamics for a body in elliptic orbits," *the Conference on Bluff Body Wakes and Vortex-Induced Vibration*, Washington, DC, USA, paper number 18, 1998.
- [14] D. Jeon and M. Gharib, "On circular cylinders undergoing two-degree-of-freedom forced motions," *Journal of Fluids and Structures*, vol. 15, pp. 533–541, 2001.
- [15] G. Reid, "On the application of active open-loop and closed-loop controls on a circular cylinder in the presence and absence of a free surface," Ph.D. dissertation, Memorial University of Newfoundland, St. John's, Canada, 2010.
- [16] L. Baranyi, "Numerical simulation of the flow around a circular cylinder following a figure-8-like path." ASME, 2010.
- [17] S. C. R. Dennis and G. Z. Chang, "Numerical integration of the Navier-Stokes equations, Technical Summary Report No. 859," *Mathematical Research Center, University of Wisconsin*, 1969.
- [18] —, "Numerical solutions for steady flow past a cylinder at Reynolds numbers up to 1000," *Journal of Fluid Mechanics*, vol. 42, p. 471489, 1970.
- [19] W. M. Collins and S. C. R. Dennis, "Flow past an impulsively started circular cylinder," *Journal of Fluid Mechanics*, vol. 60, pp. 105–127, 1973.

- [20] H. M. Badr and S. C. R. Dennis, "Time-dependent viscous flow past an impulsively started rotating and translating circular cylinder," *Journal of Fluid Mechanics*, vol. 158, pp. 447–488, 1985.
- [21] H. M. Badr, M. Coutanceau, S. C. R. Dennis, and C. Menard, "Unsteady flow past a rotating circular cylinder at Reynolds numbers 10^3 and 10^4 ," *Journal of Fluid Mechanics*, vol. 220, pp. 459–484, 1990.
- [22] S. C. R. Dennis, P. Nguyen, and S. Kocabiyik, "The flow induced by a rationally oscillating and translating circular cylinder," *Journal of Fluid Mechanics*, vol. 407, pp. 123–144, 2000.
- [23] F. Mahfouz and H. Badr, "Flow structure in the wake of a rotationally oscillating cylinder," *Transactions of the ASME: Journal of Fluids Engineering*, vol. 122, pp. 290–301, 2000.
- [24] S. Kocabiyik, F. M. Mahfouz, and Q. Al-Mdallal, "Numerical simulation of the flow behind a circular cylinder subject to small-amplitude recti-linear oscillations," *Advances in Engineering software*, vol. 35, pp. 619–631, 2004.
- [25] K. P. Lawrence, "Computation of unsteady viscous incompressible flow around an obliquely oscillating circular cylinder using a parallelized finite difference algorithm," Master's thesis, Memorial University, Newfoundland, Canada, 2004.
- [26] Q. Al-Mdallal and S. Kocabiyik, "Rotational oscillations of a cylinder in cross-flow," *International Journal of Computational Fluid Dynamics*, vol. 20, no. 5, pp. 293–299, 2006.

TABLE I
THE EFFECT OF OSCILLATION AMPLITUDE, A , ON THE FLUID FORCES (DRAG, LIFT AND MOMENT) FOR THE CASE $R = 200$, $f/f_0 = 1.0$ AND $0.1 \leq A \leq 1.0$.

A	Lift force			Drag force			Moment					
	$C_{L,max}$	$C_{L,min}$	$C_{L,rms}$	$\overline{C_L}$	$C_{D,max}$	$C_{D,min}$	$C_{D,rms}$	$\overline{C_D}$	$C_{M,max}$	$C_{M,min}$	$C_{M,rms}$	$\overline{C_M}$
0.1000	1.3580	-1.3032	0.6960	0.0232	1.5869	1.1139	1.3428	1.3348	1.9570	-1.7281	0.8831	0.0322
0.2000	2.1158	-2.0267	1.1166	0.0960	1.8545	0.9465	1.4214	1.3937	2.8733	-2.6373	1.2704	0.0327
0.3000	3.0350	-2.5990	1.5052	0.0391	2.3558	0.6907	1.4985	1.4406	3.5969	-4.8070	1.5445	0.0882
0.4000	3.6844	-3.0879	1.9794	0.2102	2.8478	0.4796	1.6195	1.5117	3.1749	-5.4108	1.9392	-0.0863
0.5000	4.3369	-3.9330	2.4228	0.2044	3.7320	0.2096	1.8698	1.6780	4.4718	-7.4654	2.5923	0.0302
0.6000	5.0978	-4.5240	2.8474	0.3462	4.3090	-0.1636	2.0216	1.7570	5.2597	-7.8356	2.9664	0.0682
0.7000	5.9344	-5.0652	3.2501	0.3692	5.3636	-0.4984	2.3997	1.9793	7.1169	-10.1640	3.7625	0.1816
0.8000	6.8014	-5.4866	3.5814	0.4684	6.0216	-1.1067	2.6830	2.1239	8.9321	-10.0872	4.1009	0.1308
0.9000	7.3516	-5.8403	4.1190	0.7489	6.6046	-1.8099	2.7528	1.9591	10.9620	-12.3710	4.6248	-0.0388
1.0000	8.0495	-6.0262	4.3558	0.8848	7.6586	-2.6941	3.1864	2.0481	9.2758	-12.4374	5.1515	-0.2012